Bulletin of the Seismological Society of America, Vol. 95, No. 1, pp. 1–17, February 2005, doi: 10.1785/0120030261

Powerful Low-Frequency Vibrators for Active Seismology

by A. S. Alekseev, I. S. Chichinin, and V. A. Korneev

Abstract In the past two decades, active seismology studies in Russia have made use of powerful (40- and 100-ton) low-frequency vibrators. These sources create a force amplitude of up to 100 tons and function in the 1.5–3, 3–6, and 5–10 Hz frequency bands. The mobile versions of the vibrator have a force amplitude of 40 tons and a 6–12 Hz frequency band. Recording distances for the 100-ton vibrator are as large as 350 km, enabling the refracted waves to penetrate down to 50 km depths. Vibrator operation sessions are highly repeatable, having distinct "summer" or "winter" spectral patterns. A long profile of seismic records allows estimation of fault zone depths using changes in recorded spectra. Other applications include deep seismic profiling, seismic hazard mapping, structural testing, stress-induced anisotropy studies, seismic station calibration, and large-structure integrity testing. The theoretical description of the low-frequency vibrator is given in the appendices, which contain numerical examples.

Introduction

The goal of this article is to give a short review of a Russian research program dealing with the development and application of powerful low-frequency vibrational sources. There is increasing interest in the use of such sources for deep seismic profiling, seismic hazard mapping, structural testing, and various seismological applications in the United States, and these sources could be especially important for the recently initiated EarthScope project.

In the 1980s, several institutes of the Siberian Branch of the Russian Academy of Sciences developed a long-term seismic research program based on the use of vibrational seismic sources. A low-frequency eccentric vibrator (LEV) capable of producing a 100-ton force was designed, built, and tested. The operational frequencies of this LEV can be tuned to several frequency bands (1.5–3 Hz, 3–6 Hz, 5–10 Hz). The duration of a vibrator operation may be of any length, starting from 5 min; in practice, the average duration is about an hour. See Active Seismology Studies and the Appendixes for information about this source in more detail.

The use of vibrational sources includes several important applications:

1. Seismic monitoring of seismically active regions in search of earthquake precursors,
2. Deep seismic profiling for crust and upper mantle studies,
3. Station calibration for nuclear explosions monitoring purposes,
4. Seismic hazard mapping for the estimation of potential seismic impact to buildings,
5. Geodynamic processes studies,
6. Diagnostics of the integrity of dams, bridges, large industrial facilities, and nuclear power plants,
7. Soft soil compaction,
8. Enhanced oil recovery stimulation studies.

To solve these problems, new geotechnologies based on the use of powerful low-frequency vibrators have been created (Alekseev *et al.*, 1997a, 1997b, Alekseev *et al.*, 2002).

Powerful Low-Frequency Eccentric Vibrators

From 1970 to 1990 the hydraulic vibrators with force amplitude of 10–15 tons and an 8–150 Hz frequency band were frequently used in the United States. This stimulated similar development in the USSR, with the first seismic vibrators there also driven by hydraulic motors. However, the Russian designers of the seismic vibrators (Chichinin, Yushin, Kulakov, Zuev) concluded (Chichinin and Okunev, 1975) that for mobile vibrators working on the ground in the low-frequency band, the preferred source is the LEV.

We know from experience that for eccentric vibrators used in road construction, the following empirical law holds: If we need to provide a force with amplitude of N tons, then an N (kW) power supply is needed. For the hydraulic vibrator built on the piston-cylinder principle, a $10 \cdot N$ (kW) power supply is needed. This results from a special property of LEV, where the rotating masses provide energy recuperation. During the vibrational compaction of pavement, the pressure on the ground by the source should be strong enough to cause permanent deformation. If this pressure is decreased, then the power usage of the LEV should be even smaller than that given by N tons $\rightarrow N$ kW.

Initially, a seismoexploratory eccentric vibrator (Vibrolocator) with a force amplitude of 10 tons and frequency

range of 10–70 Hz was developed, under the initiative and direction of I. S. Chichinin, for oil and gas prospecting, using both P and S waves (Chichinin and Okunev, 1975; Yushin, 1981). The force of the vibrator may be oriented in both the vertical and horizontal directions by using electronic controls. Such an orientation is fairly simple to achieve in an eccentric source. It was intended that a group of Vibrolocator sources would be used simultaneously, to ensure the synchronization of three to five sources with none of them varying from the phase of the sweep signal by more than 10°. The eccentric force chambers were located on the two vibroplatforms, with one of them in front of a tractor and the other behind it. The hydraulic "legs" of the tractor pressed these platforms to the ground.

In 1976–1978, a vibrator for active seismology, with a force amplitude of 100 tons and a frequency range of 1.5–3 Hz, was made in the institutes of the Siberian Branch of Russian Academy of Sciences. Its system of precise frequency and phase control was identical to that of the Vibrolocator. For this source, the inertial mass M_i $3.5 \cdot 10^3$ kg, the distance of mass center from rotation axis $U_i^{(\max)} = 0.4$ m, and source parameters are related by equations (19) and (20) in Appendix B.

For deep seismic profiling (DSP) purposes, the aforementioned vibrator was redesigned for the frequency range of 5–10 Hz by modifying the core masses. As a result, an amplitude of $F_o = 100$ tons was reached at the frequency 10 Hz, whereas at a frequency of 5 Hz the amplitude was just 25 tons, since the core masses were not modified during the session. Operation thus relies on the area of the radiating vibroplatform $S_{pl} = 4 \cdot 5$ m^2 being chosen so that the mass of the source $M_{pl} \approx 120 \cdot 10^3$ kg with ground stiffness (K_{gr}) would resonate at a frequency of about 5–6 Hz. (In this case, the restraining mass $M_{pr} = 0$. Such vibrator design is discussed in Appendix C, case V3. Stiffness, K_{gr}, is given by equation 17.)

Because of the resonant motion of the mass M_{pl} with the ground, represented by "spring" K_{gr}, the force F_{gr} acting on the ground increases; in the range 5–6 Hz, the force approaches 100 tons, rather than being only 25 tons. As a result, a seismogram recorded from this vibrator had a more or less even spectrum in the range 5–6 to 10–12 Hz. Examples of such seismograms are shown in Active Seismology Studies.

A photograph of a 100-ton vibrator is shown in Figure 1. Columns standing on the vibroplatform support a metal panel and on this panel sits a mass of about $100 \cdot 10^3$ kg. Hence, the net weight that acts on the ground is about $M_{pl} \approx 120 \cdot 10^3$ kg. It follows that the amplitude of the pressure acting on the ground is no larger than 0.6 kg/cm^2. (This pressure is similar to the pressure exerted by a shoe of a standing man.) As a result, the vibroplatform does not compact or otherwise deform the medium on which it acts, which accounts for the repeatability of experiments.

Currently, one stationary 100-ton vibrator is installed at the Bystrovsky test site (not far from Akademgorodok), another is close to the town of Babushkino, near Lake Baikal, and the third vibrator is set in the Krasnodarsky Region.

The 100-ton source described previously is a stationary structure, but for a number of problems it is necessary to have a mobile vibrator. Hence, a 40-ton mobile vibrator (Fig. 2), an analog of the 100-ton vibrator, has been designed.

In the previously mentioned LEVs, the quantity $U_{io} \cdot M_i$ (see Appendix B) was unalterable during the session.

The 100-ton vibrator has the total weight of 120 tons with 4 m by 4 m ground platform and can be disassembled for transportation. It consumes 100 KW of power. The 40-ton vibrator has the total weight of 50 tons with 3 m by 4 m ground platform and also can be disassembled for transportation. It consumes 40 KW of power.

The U.S. Network for Earthquake Engineering Simulation (NEES) consortium has developed hydraulically powered low-frequency vibrators "Liquidator" (with the total weight of 27 tons and 2.4 m^2 platform area) and "T-Rex" (29 tons, 2.4 m^2). The comparison of ground forces achievable by those sources (http://nees.utexas.edu/equipment

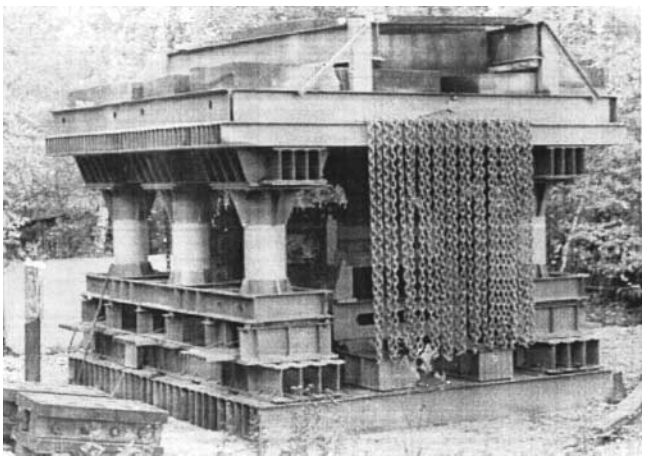

Figure 1. A view of the 100-ton vibrator (Alekseev *et al.*, 2002).

Figure 2. A view of the 40-ton vibrator (Alekseev *et al.*, 2002). 1, 2, 3, platform elements; 4, loading mass, M_{pr}; *5*, transmission; 6, electric motors.

.htm) is given in Table 1, where similar data are also given for 100-ton LEV for 12, 10, 6, and 3 Hz regimes.

Propagation Distances and Repeatability

The propagation distance of a powerful LEV signal is illustrated in Figure 3, where seismograms recorded at 20, 96, 170, and 286 km are presented. Locations of the source and recording profiles are shown on Figure 4. In this experiment the vibrator was working in the 5–10 Hz frequency band, with the point of excitation on the Bystrovka vibroseismic test field, situated on the bank of Obski reservoir, about 70 km southwest of Novosibirsk. The recording lines were oriented in west–south directions, and the longest one extended from Bystrovka to Lake Chany, located at a 286-km offset. The duration of the vibrational session was 45 min.

The first arrivals on the seismograms recorded at the 170- and 286-km offsets belong to waves reflected from the Moho discontinuity, which has a depth of about 40 km. High-amplitude shear (*S*-) waves arrive much later. At small offset distances, the first arrivals consist of waves refracted by the Earth's crust. The first 200 m of depth in the region are composed of sediments, whereas the rest of the crust depth is composed of a crystalline basement with a complex structure. For comparison and discrimination purposes, a surface explosion with 5 tons of TNT equivalent was also made, in the Iskitim quarry close to the Bystrovsky test site. Seismic signals from this explosion were recorded by the same stations at a 286-km offset. The obtained record had the same structure as in Figure 3, although the signal-to-noise ratio on the explosion seismogram was lower. The refracted waves, which are cross-correlated with the sweep signal for transformation into impulse form, have a recording distance $L = 300$–350 km that is sufficiently large for the illumination of the crust at all depths down to $h = 40$–60 km–the maximum depth penetration of the refracted wave can be estimated using the expression $h \approx L/(4–7)$.

Studies on the repeatability of the vibration session are described in Emanov *et al.* (1999). The vibrator from the Bystrovsky test site and the seismological station "Novosibirsk" (at the town Kluchi, and located 49.1 km from the source) were used. This station has a thermostatic pavilion with a three-component seismometer SK-1P placed on a concrete foundation sitting on bedrock. The recording was made by the digital seismic station Alpha-Geon, which recorded displacement velocity.

The systematic recording of the vibroseismic signal by the station "Novosibirsk" was started in the summer of 1996. Every one-day-long experiment consisted of up to four consecutive sessions. The interval between experiments varied from one day to two weeks. Figure 5 shows seismograms and spectra recorded in the period from January 1997 to June 1998 (Emanov *et al.*, 1999).

It is clear that the obtained records can be conventionally subdivided into summer (June–November) and winter (January–March) periods.

Table 1
Ground Force for Different Vibrators

	Frequency (Hz)								
	1	2	3	6	8	10	12	16	20
"Liquidator"	4.45	10	10	10	10	10	10	10	10
"T-Rex"	0.18	0.74	1.67	3.8	11.8	18.5	26.7	26.7	26.7
100-ton LEV									
Regime "12"	0.7	2.8	6.25	25	44	69	100		
Regime "10"	1	4	9	36	64	100			
Regime "6"	2.8	11	25	100					
Regime "3"	11	44	100						

The seismograms recorded in the summer, when the upper soil was not frozen, have very high repeatability and are visually identical. From the start of November 1997, there were stable freezing temperatures reaching -30°C, and the soil under the vibrator was freezing rapidly. Despite this freezing, the vibrator emission has a summer character until November, likely because of slow propagation of temperature waves in the ground.

In January 1997 (and in January 1998), the emission was drastically different from that which had been observed previously. The winter seismograms recorded in January–March for both 1997 and 1998 have high repeatability as well.

These observations show that vibrator emission changed from summer to winter emission types in the December–January transition. Then, the winter type of emission continued until mid-April. The spring of 1997 progressed very slowly, and positive temperatures stabilized as late as in May. The vibrator reverted back to the summer emission type by the beginning of June.

It is remarkable that both the summer and winter seismograms recorded in different years are visually identical. It was assumed that the seasonal changes in the vibrator field resulted from soil freezing under the vibroplatform; hence, the vibrator was placed into a specially made large and warm insulating basement. Still, summer and winter seismograms were different, although the soil under the vibrator was not frozen. Consequently, the wave field was affected not just by changes of the soil under the vibrator, but also by changes in the surrounding ground. We should note that the travel times of the first arriving waves did not reveal any seasonal changes. Spectra of summer and winter seismograms (Fig. 5b) differ in the following manner: the summer amplitude spectra begin from 6 Hz, whereas the winter amplitude spectra begin from 7 Hz. This difference characterizes changes in vibrator emission content during the period under consideration.

The results from these experiments lead us to conclude that experiments for which repeatability is important should be planned for either summer or winter seasons.

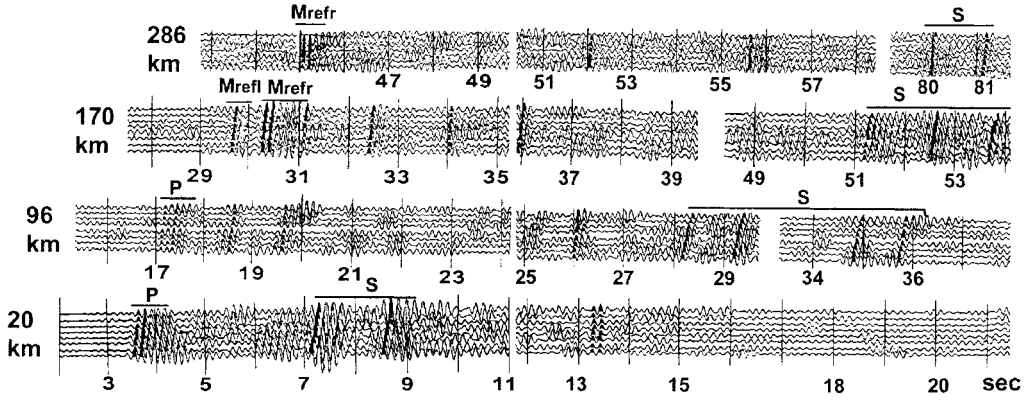

Figure 3. Seismograms recorded at 20, 96, 170, 286 km offset distances from a 100-ton vibrator (Alekseev *et al.*, 1982). For the 286 km offset, the duration of the vibrational session was 45 min. M_{refr} and M_{refl} are, respectively, the refracted and reflected waves from the Moho discontinuity. In the region of the experiment the Moho discontinuity is approximately 40 km deep.

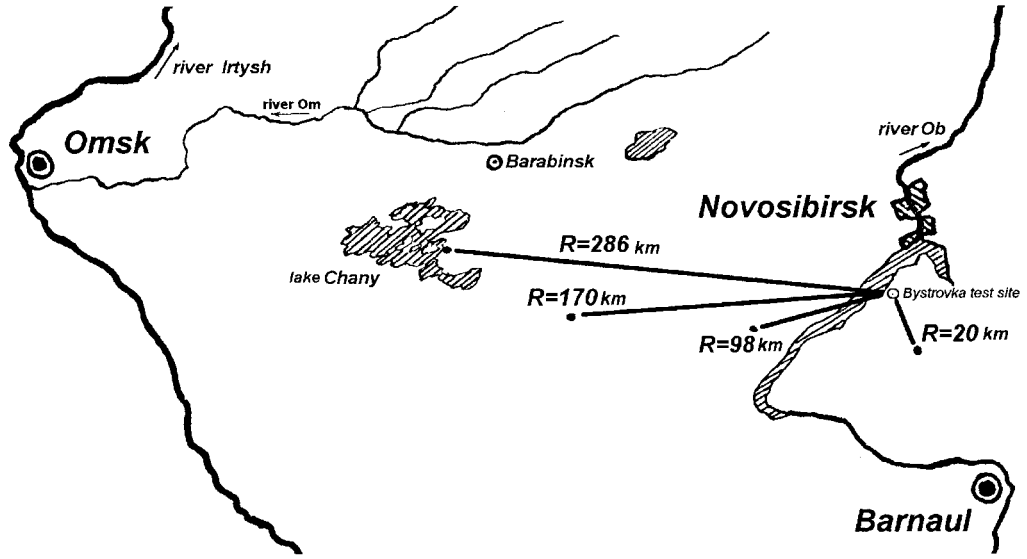

Figure 4. Locations the vibrator and recording profiles for data shown in Figure 3.

Active Seismology Studies

One significant application of a highly repeatable seismic source involves monitoring changes in Earth's crust in search for earthquake precursors. Our seismically active zone monitoring research explores the theory of Alekseev *et al.* (2001), which predicts a significant rearrangement of microfractures in the zone of a future earthquake. The fractures, which are initially spread in a large rock volume, have a tendency to be localized in the zone of the future fault; the rearrangement of fractures before earthquakes can happen in an abruptly discontinuous way. It is assumed that such processes take place mostly inside existing fault zones. Several experiments were conducted that were aimed at determining whether it is possible to use vibroseismic sources for locating fault zones and estimating their depths (Emanov *et al.*, 1999).

A 100-ton vibrator was placed in the area of Babushkino, 1 km from the shoreline of Lake Baikal. The observation profile was 125 km long with 20 km spacing between stations and oriented across the deep faults of the Chamar-Daban mountain range and the Gusinoozerskaya Valley. At all recording points, the 10-channel seismograms were recorded with a high signal-to-noise ratio.

Figure 6 shows the amplitude spectra of the refracted direct *P* wave for different stations. Each station is represented by spectra from two channels. A significant feature of the these data is the presence of different spectral widths for the same source signal. At a distance of 7 km from the vibrator, the signal of the refracted wave has high amplitudes

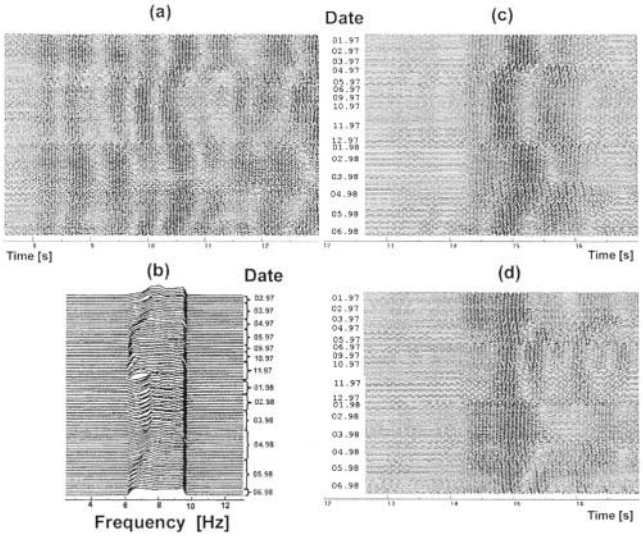

Figure 5. LEV repeatability study for the January 1997–June 1998 period. The seismograms are recorded at 1–2 week intervals (Emanov *et al.*, 1999) by a three-component (east–west, south–north, *z*) receiver located on top of the bedrock, in the thermostatic pavilion of the seismological station "Novosibirsk." The source-receiver distance is 44.1 km. Panel (a) shows vertical component, panels (c) and (d) correspondingly show horizontal components in east–west and south–north directions. *P* waves arrive in the 8–9 s interval, and *S* waves can be seen for $t > 14.5$ s. The interval 9–14.5 s contains converted *P-S* phases. Panel (b) shows spectra of vibroseismic oscillations at a depth of 3 m under the vibrator for the February 1997–June 1998 period.

for the entire vibrator frequency band. At 20 km only the low-frequency part of the original spectrum is present in the data. The corresponding observation point is located directly behind a deep tectonic fault, which is oriented parallel to the Chamar-Daban mountain range. Remarkably, at the next recording point, at 38 km offset, the spectrum widens again. This frequency content change suggests that the corresponding seismic ray goes to this point without crossing the fault zone and that, at a depth of about 5 km, rocks have small attenuation coefficient.

The first fault of the Gusinoozerskaya Valley crosses the observation profile between the stations at 38 km and 55 km. The second fault of the same valley crosses the observation profile between the stations at 55 and 85 km. This circumstance reveals itself in the shifting of spectral content for the records from 55 km and 85 km points toward the low frequencies. The ray travels to the 93 km recording point along the relatively undamaged rock, and the corresponding spectra has a wide frequency range.

The results of these experiments lead to the following conclusions: One seismic vibrator is capable of illuminating a seismically active area with a 200–300 km radius. The observation should be made in a specially selected set of points, considering actual configuration of the fault systems. For long-term prediction stations, the interval between successive recordings can be as long as half a year (during the summer or the winter). Utilizing the high repeatability of the summer and winter seismograms, surveys can be performed by using a relatively small number of stations.

Experiments with this 100-ton vibrator at Lake Baikal were recently continued, and new data are currently being processed.

Deep Seismic Profiling

Using the 100-ton vibrator from the Bystrovsky test field, observations were made on two orthogonal profiles: Bystrovka-Aleysk, 360 km long, Bystrovka-Prokopievsk, 225 km long, with 5–20 km spacing, and Bystrovka-Degelen, 600 km long (Alekseev *et al.*, 2002). Travel-time curves for the two orthogonal profiles are presented in Figure 7. The Bystrovka-Degelen profile was extended further in a monochromatic (single-frequency) mode. In this mode, the maximum distance for reliable recording of oscillation amplitude and phase is at least 1400 km. The recording of monochromatic signals was done on the shore of Lake Balkhash in East Kazakstan.

Using the transportable 40-ton vibrator (of a design similar to the 100-ton vibrator), the deep profiling Common Deep Point (CDP) seismic survey was conducted along the line between Bystrovka and Tashtagol (100 km long) and the line between Magadan and Kolyma (300 km long) (Alekseev *et al.*, 2002).

The data allow stable correlation of wave arrivals of different kinds and their interpretation. In Figure 8, the reduced travel times of *P* waves are shown for the 250 km Bystrovka-Zalesovo-Novokuznetsk profile, which were attributed to waves refracted from the Earth's crust and also to waves refracted and reflected from the Moho discontinuity (Glinsky *et al.*, 2002).

Seismic Station Calibration

Accurate monitoring of nuclear testing is an important practical problem, which requires discrimination between a small underground nuclear explosion from a natural small-amplitude earthquake. Accurate information about the location of any of these events allows such problems to be solved rather reliably.

To detect a nuclear explosion, seismic recorders must be installed at sites suitable for determining the explosion location, but this by itself is not enough to achieve the goal. The accuracy of epicenter location determination substantially depends on knowledge of the crustal structure in the region. The technology designers believe that crust studies (down to 50–70 km depths) in such regions should be performed with powerful LEVs (Alekseev *et al.*, 2002). This is easier, faster, and cheaper than using multiple explosion sources equivalent to 3–5 tons of TNT. A comparison of seismic data records produced by the previously mentioned

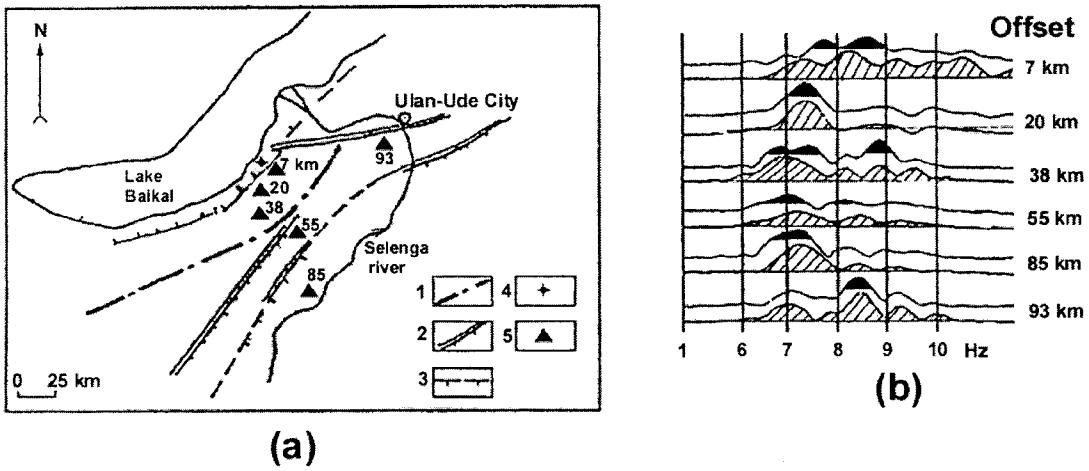

Figure 6. Changes in the wave spectra due to their propagation across the tectonic faults (Emanov *et al.*, 1999). (a) Experimental plan view. 1, main geological boundaries; 2, general faults; 3, normal faults; 4, LEV; 5, recording points with offset distances (km). (b) Amplitude spectra of the recorded waves for two channels recorded at 7, 20, 38, 55, 85, and 93 km offsets.

explosion source and the 100-ton vibrator for the reversed far offset profiles (≈ 220 km) is shown in Figure 9. Although the seismograms in Figure 9a and b differ in some details, their main features are similar.

A seismic station calibration test was performed at the Bystrovsky site. Several actual explosions were used as seismic events: the industrial explosions from Kuzbass quarries and the explosion of 100 tons of TNT on 29 June 2000, which was carried out to destroy a shaft in Degelen, at one of the former nuclear test sites in Semipalatinsk. The data from these measurements show that the coordinates of the seismic event can be determined much more accurately if information about crust structure of the region is used (Alekseev *et al.*, 2002).

Seismic Hazard Mapping

Seismic hazard mapping can be performed when general knowledge about regional seismicity already exists. It solves the problem of evaluating the local soil response to incoming seismic waves.

Among the many different methods of seismic hazard mapping, the most representative is a comparison of the oscillation amplitudes for small-energy earthquakes. An increase of amplitudes, by a factor of two, corresponds to a one-unit increase of local seismic magnitude. It is assumed that surface-amplitude ratios do not depend on the magnitude of the events.

This earthquake method is compromised by the irregularity of microseismic events when the time of the incoming event is unpredictable. In urban regions, the robust recording of incoming signals is difficult because of increased background noise. In contrast, if a powerful LEV is used, the timing of recording can be perfectly coordinated. A 50–100 ton vibrator placed at any central point of a seismically active region is capable of illuminating a territory with radius of 100–200 km.

Geodynamic Processes Studies

High repeatability and accuracy of phase control (less than 1°) allow powerful low-frequency vibrators to be used for geodynamic studies. Glinsky *et al.* (1999) show examples of data recorded at 356 and 430 km from a 100-ton vibrator. These records were obtained every 2–3 hr over 4 days. The data revealed 24- and 12-hr periodicity for both amplitudes and phases. Figure 10 shows a comparison between these variations with gravimeter data. Glinsky *et al.* (1999) conclude that the observed changes are likely to be induced by tidal stress changes, which are estimated to be in the 10^{-5}–10^{-6} range.

Integrity Diagnostics of Large Structures

To test the integrity of large structures, seismic receivers should be placed at a set of reference points with the vibrator source located at a substantial distance from the structure. Recorded oscillations can be converted into impulse form by cross-correlation with the source sweep. In the first arrivals of the seismogram, *P* waves can be observed, usually with an almost vertical incidence. The response of the structure to the *P* waves is almost the same as it would be to a vertically acting force. In the later arrivals, shear *S*-waves can be observed, with high-amplitude horizontal x and y components. The character of the recorded signals here resembles the structure's response to horizontal displacements.

The technology of long-session vibrosignal processing helped to develop the original microseismic applications. Figure 11 shows a seismogram recorded by receivers placed

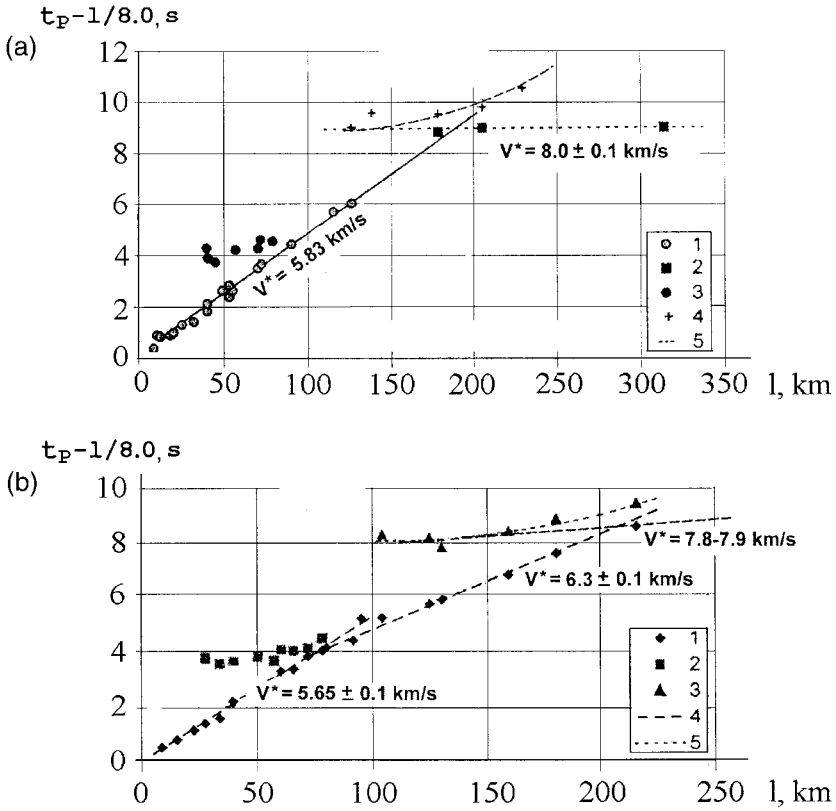

Figure 7. Reduced travel times of P waves excited by a 100-ton LEV for the profiles I-I (a) and II-II (b). (a) 1, first arrivals of waves from the earth's crust boundaries; 2, waves refracted from Moho discontinuity; 3, 4, reflected waves P^{K}_{refl} and P^{M}_{refl}, correspondingly; 5, averaging lines. (b) 1, refracted P waves; 2, 3, reflected waves P^{K}_{refl} and P^{M}_{refl}, correspondingly; 4, averaging lines; 5, theoretical travel-time curve of P^{M}_{refl} wave for the medium model with parameters V = 6.4 km/s, H = 43 km (Alekseev *et al.*, 2002).

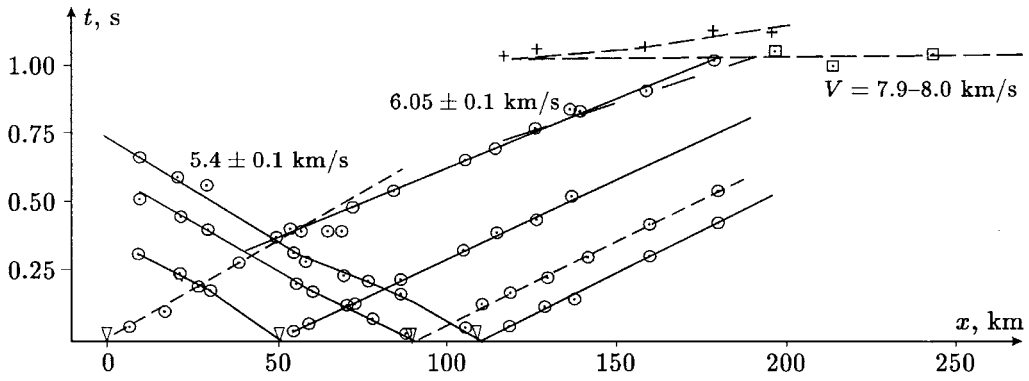

Figure 8. Reduced travel times of P waves for the 250 km profile Bystrovka-Zalesovo-Novokuznetsk. Shown are ⊡, waves refracted from the Earth's crust boundaries; ⊙, waves refracted from Moho discontinuity; and +, waves reflected from Moho discontinuity (Glinsky *et al.*, 2002).

along corridor 521 of the dam for the Sayano-Shushenskaya hydro-power plant. The height of the dam is 200 m, the length is 1074 m. In the concrete body of the dam, there are corridors at a 27 m vertical interval. Corridor 521 is 521.15 m above sea level, whereas the lowest corridor of this dam is 308 m above sea level.

To obtain seismograms of the type shown in Figure 11, one would normally require hundreds of three-component seismometers, which are difficult and expensive to install. In this case, a different method was used, in which just one three-component receiver stays at the same point, whereas several other identical seismometers are moved from point to point. The source of the seismic signal is mechanical noise of different kinds. It was found that the auto- and cross-correlation functions of these oscillations stabilize their shape after 5–7 min of recording. Therefore, two to three persons can conduct the entire survey of the large structure in several days without any interruptions in operations.

At the processing stage, these records are sewn together by using the method developed by Emanov *et al.* (2002).

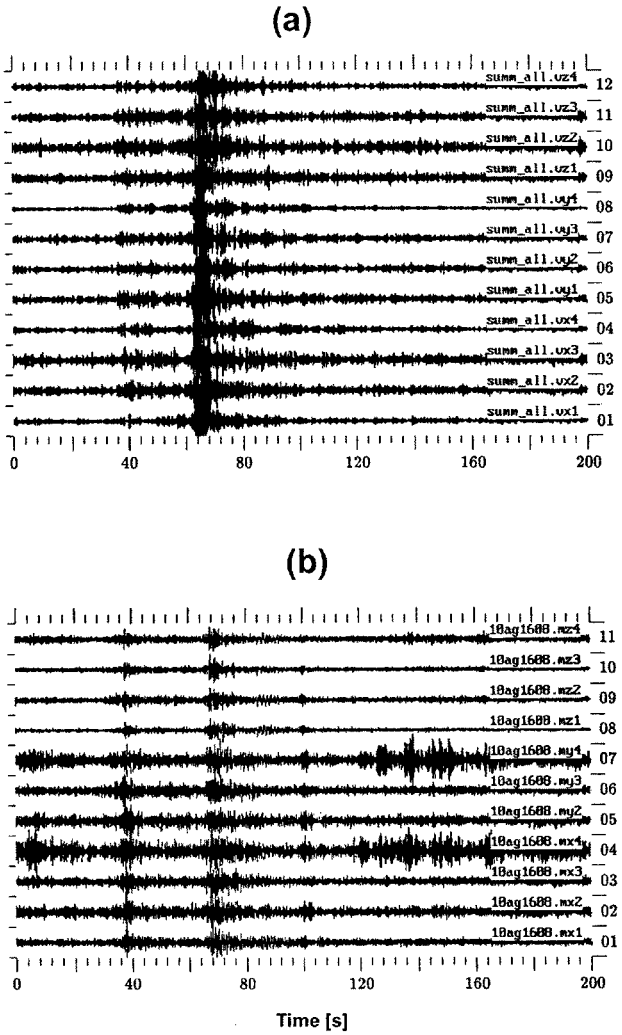

Figure 9. Comparison of seismic data records at 250–253 km offset produced by 100-ton vibrator Bystrovka-Bachatsky (a) and the explosion Bachatsky-Bystrovka (b) for 6.25–9.57 Hz pass filter (Glinsky *et al.*, 2002). Note that the vibrator generates more intensive *S* waves than the *P* waves.

The resulting traces are equivalent to those of an installation with a large number of receivers. Such records allow easy extraction of the first ten modes and of modes shaped in lateral and vertical directions. The records also contain wavefronts incident to and reflected from the edges of the dam. The obtained traces closely resemble those of seismograms traditionally recorded in vertical seismic profiling surveys.

The seismogram in Figure 11 is a *y* component of the first eigenfrequency. It has a maximum at 2 Hz with apparent velocity $V^* = 1342$ m/s. The *y* axis is horizontal and oriented across the dam. Experiments show that the apparent velocities of the different modes can be significantly different. According to Emanov *et al.* (2002), the records from Figure 11 correspond to flexural oscillations of the object. The waves reflected from the edges of the dam characterize the rigidity of the dam's connection with canyon walls. The differences in the apparent velocities of the various modes characterize the stiffness of dam's contact with the bedrock below.

The flexural modes are important characteristics for the design of mechanical assemblies. However, in many practical cases, the sizes of these objects are much smaller than wavelengths of vibrational frequencies. It seems that the general oscillation pattern and the wave propagation data for large objects reported by Emanov *et al.* (2002) are among the first of their kind.

The two methods that use a large vibrator and microseismicity are complementary. To determine the actual deformation of the structure, receivers should be placed at very short intervals ($\Delta x \approx 3 - 5$ m). For this purpose, use of a vibrator is not necessary, and just microseismic events can be utilized, which also can be used for the characterization of the main oscillation modes. But to determine how different points of the structure will oscillate relative to a point near the structure, we must to have a controlled source. It is very difficult to use natural sources, since the background noise of the power plant is high and only records for strong earthquakes can be registered there. Also, the broad application of this technique to other large structures would be hampered by uneven spatial distribution of earthquakes near these structures.

Prospectives for Active Seismology

Seismic hazard mapping and structural testing require a vibrator with a working range starting from 1.5 Hz. This range may be achieved by a replacement of the core masses, but this is not very convenient. Hence, it is a primary goal of the designers to expand the working range of the source in the direction of lower frequencies. The higher-frequency limit will also be expanded up to 15–20 Hz.

Earlier, it was stated that for the exploration of the earth's crust, it is sufficient to have a vibrator of the 50- to 100-ton mass class. Yet there are other considerations: the verification of a number of hypotheses concerning the structure and formation of the earth requires that the accuracy of knowing of *P*- and *S*-wave velocities at great depths be increased 10-fold (Artushkov *et al.*, 1974).

Earthquakes do not provide a sufficiently dense coverage of the earth (because of the irregularity of seismicity patterns), but use of powerful vibrators can significantly improve the coverage. The question arises: what kind of vibrator is required to explore the entire lithosphere (to 70–100 km), mantle (to 3000 km), and the core? Chichinin (1990) answered this question in the following way: Figure 12 shows graphs of the decay of *P*-wave amplitudes that were compiled based on earthquake data collected by a combined expedition of the Institute of Earth Physics of the Academy of Sciences of the USSR and USGS.

It can be seen from the graphs that *P*-wave amplitudes decay 5–8 times in the interval 300–700 km. It follows that

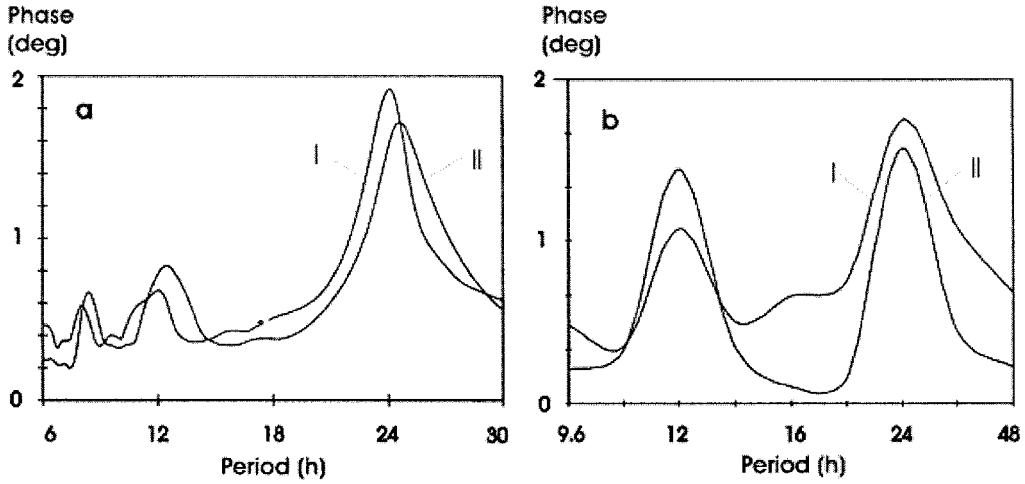

Figure 10. Spectra of vibrosignal phase variations (I) and tidal related gravitational force (II): (a) 1996 data for 430 km offset; (b) 1997 data for 356 km offset.

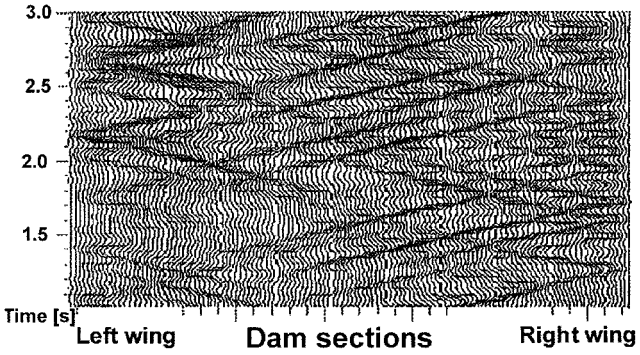

Figure 11. Seismograms recorded in the gallery of the Sayano-Shushenskaya hydropower dam (Emanov *et al.*, 2002). The gallery is inside of the dam and extends for the whole dam length (1080 m). The *y*-component recorders are oriented along the river flow. Clearly visible are the flexural waves with $V^* = 1342$ m/s velocities which are incident and reflected from both sides of the dam.

to achieve a signal-to-noise ratio comparable with that of the seismograms in Figure 3, we will need a vibrator of amplitude 500–800 tons for vibration session lasting 1 hr. In this case, depths up to 200 km will be illuminated. To get a seismogram at a distance of 10,000 km (i.e., an illuminated depth of up to 3000 km), a 10-kiloton force amplitude is required.

A vibrator may also be used to relieve internal pressures in mines and other underground structures. This would require a source with an amplitude of 1–5 kilotons (Krauinsh *et al.*, 1990). It should be noted that there exist accurately computed designs of a low-frequency vibrator in the kiloton class that may function in a flooded mine shaft or in the sea. However, such sources have the peculiarity that although the amplitude they can generate is large, the radiated power is comparatively small. The recuperation of energy in such vibrators is achieved through the low attenuation of an air bubble if the volume amplitude of its oscillations is less than 10% of its total volume. During a session, the resonant frequency of the air bubble may be varied by changing its volume, that is, by releasing a fraction of the air into the water. The power usage of the source will be about equal to the power radiated by its elastic waves.

For example, suppose that a source with an air volume of 6 m^3 is placed on a depth of 47 m with a resonant frequency of 4 Hz. It will produce the same amplitude in the far field as a previously mentioned ground source of about 5 kilotons, whereas the radiated power will be only 4 kilowatts.

Conclusions

A wide array of seismological problems involving crustal studies (depths down to 40–60 km) are solvable using vibrators with a force amplitude of 50–100 tons operating in low-frequency bands. The high repeatability of vibroseismic radiation provides the possibility of conducting new and exciting studies. These studies include detailed deep seismic profiling on long profiles made with the use of relatively small quantities of receivers, monitoring of seismically active regions, seismic hazard mapping, etc. There is good reason to believe that low-frequency seismic vibrators can help to achieve EarthScope science goals if used as controlled powerful seismic sources. This is especially important since the transportable component of USArray is designed to stay 1.5–2 years in stationary positions and will be affected by seasonal changes. The natural seismic sources recorded by this array may not be enough to provide uniform and dense enough coverage for the high-resolution inversions. The controlled, powerful sources could be very helpful in providing the necessary coverage to solve these problems.

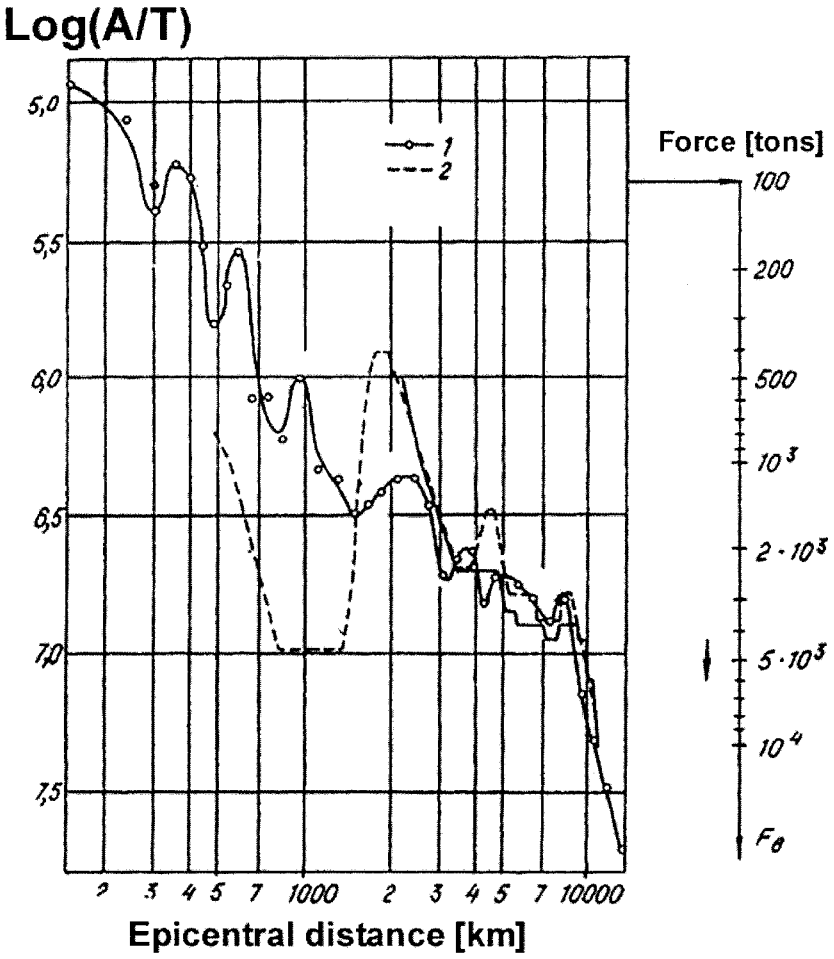

Figure 12. Amplitude of the direct *P* wave versus epicentral distance (Antonova *et al.*, 1968; Chichinin, 1990). (1) Data from the Institute of the Physics of the Earth Academy of Sciences of USSR; (2) data from USGS. Right vertical scale shows the ground vibrator force needed for recording of seismograms similar to those of Figure 1. This scale shows that if we need a 300 km distance for a 100-ton vibrator, then for the same quality of data and vibrosession duration at 10,000 km distance we need a vibrator with 10-kiloton force amplitude.

Acknowledgments

This research project has been supported by the Geosciences Research Program, Office of Basic Energy Sciences of the U.S. Department of Energy under Contract DE-AC03-76SF00098. We are grateful to Irina R. Obolentseva and Andre Kornell for their help during preparation of manuscript. Two anonymous reviewers made many helpful comments and suggestions.

References

Alekseev, A. S., B. M. Glinsky, V. V. Kovalevsky, and B. G. Mikhailenko (1997a). Problems of active seismology, in *Upper Mantle Heterogeneities from Active and Passive Seismology*, K. Fuchs (Editor), Nato ASI Series 17, 123–130.

Alekseev, A. S., B. M. Glinsky, V. V. Kovalevsky, and B. G. Mikhailenko (1997b). Problems of active seismology, in *Trans. of 2 Int. Conference "The Structure of Upper Mantle,"* 1–8.

Alekseev, A. S., N. P. Ryashentsev, and I. S. Chichinin (1982). How to take a look inside of the planet? *Nauka SSSR*, no. 3, 30–37 (in Russian).

Alekseev, A. S., A. S. Belonosov, and V. E. Petrenko (2001). On the concept of multidisciplinary earthquake prediction with the use of integral precursor, in *Problems of Dynamics of Lithosphere and Seismicity* (Collection of Scientific Papers, M., GEOS, Computational Seismology), **32,** 81–97.

Alekseev, A. S., B. M. Glinsky, I. S. Chichinin, A. F. Emanov, V. N. Kashun, V. V. Kovalevsky, and A. K. Manshtein (2002) New geotechnologies and combined geophysical methods of studying inner structure and dynamics of geospheres, *Vibrational Geotechnologies* (in Russian), Moscow, 474 pp.

Antonova, L. V., F. F. Aptikaev, R. I. Kurochkina, I. L. Nersesov, T. G. Rautian, and V. I. Chalturin (1968). *Main Experimental Dependencies of the Seismic Wave Dynamics* (in Russian), Nauka, Moscow, 288 pp.

Artushkov, E. V., A. V. Nikolaev, and I. S. Chichinin (1974). *Vibrational Cross-lighting Of the Earth* (in Russian), VINITI, Moscow.

Chichinin, I. S. (1984). *Vibrational Radiation of Seismic Waves* (in Russian), Nauka, Moscow, 224 pp.

Chichinin, I. S. (1990). On the ways of producing vibro-sources for seismic investigation of big (2–3 000 km) depths of the Earth (in Russian), in *Radiation and Reception of Vibroseismic Signals, 1*, Institute of Geology and Geophysics, Novosibirsk, 5–40.

Chichinin, I. S., and V. E. Okunev (Editors) (1975). *Vibrational Seismic Prospecting Using P- and S-Waves* (in Russian), Trudy SNIIGGIMS, Novosibirsk, 219, 138 pp.

Emanov, A. F., V. S. Seleznev, and A. A. Bach (2002). Computation of seismic waves for detail engineering seismological studies (in Russian), *Geol. Geofiz.* **43,** no. 2, 192–207.

Emanov, A. F., V. S. Seleznev, and I. S. Chichinin (1999). Seasonal changes in vibroseismic monitoring (in Russian), *Geol. Geofiz.* **40,** no. 3, 474–486.

Gamburtsev, G. A. (1959). *Fundamentals of Seismic Prospecting* (in Russian), Gostoptechizdat, Moscow, 378 pp.

Glinsky, B. M., A. F. Emanov, M. S. Khairetdinov, V. V. Kovalevsky, and V. M. Soloviev (2002). Experimental research on calibration of seismic traces, *Math. Model. Geoph., Bull. Novosibirsk Computer Center* **7,** no. 3, 25–38.

Glinsky, B. M., V. V. Kovalevsky, and M. S. Khairetdinov (1999). Interconnection of wave fields of powerful vibrators with atmospheric and geodynamic processes, *Russian Geol. Geophys.* **40,** no. 3, 431–440.

Krauinsh, P. Ya., B. S. Klimov, and I. S. Chichinin (1990). Functional scheme of kiloton class vibrosources based on usage of hydrobody elements (in Russian), in *Radiation and Reception of Vibroseismic Signals, 1*, Institute of Geology and Geophysics, Novosibirsk, 83–111.

Yushin, V. I. (1981). Design and the application results for seismic complex Vibrolocator [in Russian), in *Development of Seismic Studies of the Earth Crust and Upper Mantle in Siberia*, Novosibirsk, 94–106.

Appendix A
Typical Scheme of a Nonexplosive Surface Source

Mechanical Scheme

A typical design for a nonexplosive (impulse/vibrational) source is shown in Figure 13a. The power chamber, which generates the force F_o^o, acts on a platform with mass M_{pl} against an inertial mass M_i. The platform may (or may not) be held down by a load mass M_{pr}. The load mass M_{pr} may be disjoined from the vibrations of the platform via a spring of stiffness K_{pr}. The load masses are typically placed symmetrically about the point of action of the force F_o^o. Hence, in Figure 13a we show the load system to be symmetrical about the center of the platform.

We model the ground as a spring of stiffness K_{gr}, damper R_{gr} and attached mass M_{gr}. The net force acting on the ground is

$$F_{gr}(t) = M_i\ddot{U}_i + M_{pr}\ddot{U}_{pr} + M_{pl}\ddot{U}_{pl}, \qquad \text{(A1)}$$

where $\ddot{U}_i$, $\ddot{U}_{pr}$, $\ddot{U}_{pl}$ are the accelerations of the corresponding masses.

For the sake of simplicity, the force of gravity is neglected. Consider the case in which the platform is out of contact with the ground. In this case, $F_{gr}(t) = 0$. Let the stiffness K_{pr} go to infinity, so that the mass M_{pr} is directly connected to the platform M_{pl}. Then, $\ddot{U}_{pr}(t) = \ddot{U}_{pl}(t)$, and under the action of the power chamber ($F_o^o \neq 0$) the mass $M_{pl} + M_{pr}$ will move in the opposite direction of M_i, in other words, the functions $\ddot{U}_i(t)$ and $\ddot{U}_{pl}(t)$ will have the same form, but opposite sign. Then, $F_{gr}(t) = M_i\ddot{U}_i + (M_{pr} + M_{pl})\ddot{U}_{pl} = 0$, and therefore $-\ddot{U}_i/\ddot{U}_{pl} = (M_{pr} + M_{pl})/M_i, \ddot{U}_{pl} = -\ddot{U}_i \cdot M_i/(M_{pr} + M_{pl})$.

Consider another example. For the case in which the stiffness K_{pr} vanishes or the spring is very soft, the vibrations of the platform M_{pl} cause the spring K_{pr} to contract and expand, while the mass M_{pr} remains at rest.

Now suppose that the source is placed on the ground. To begin with, consider a source with no load mass ($M_{pr} = 0$). The platform lies on soft soil on a very soft spring of stiffness K_{g1}. Below the soil is a layer of clay with stiffness K_{g2}. At $t = 0$, the power chamber begins expanding, forcing the platform M_{pl} down and the inertial mass M_i up. The platform encounters a very soft spring, so masses M_{pl} and M_i act as if the platform were out of contact with the ground.

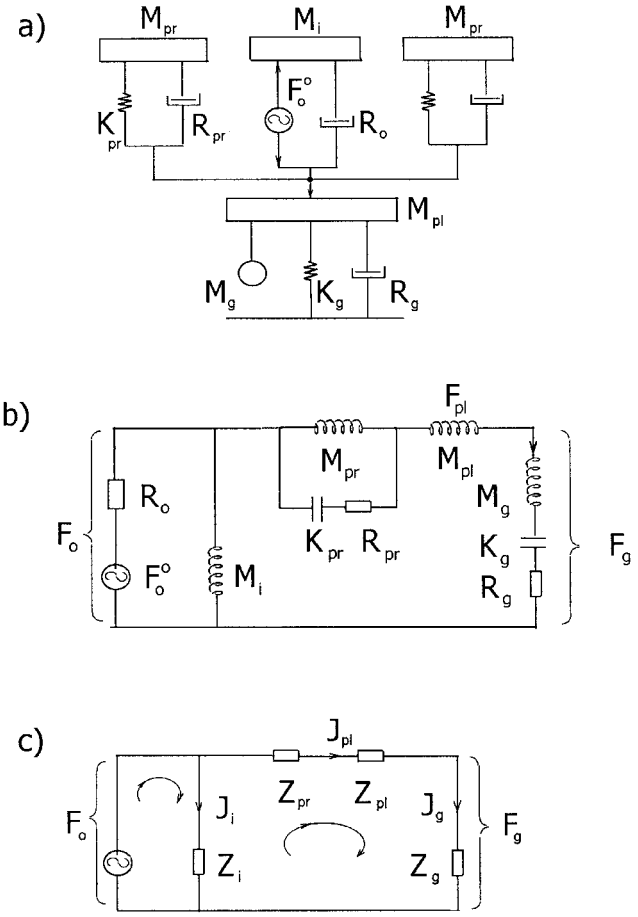

Figure 13. Typical design of surface vibrational source (Chichinin, 1984). (a) Mechanical scheme; (b) electromechanical analog scheme; (c) electrical analog with generalized impedances. F_o^o, force generated by the power chamber acting between inertial mass M_i and the platform M_{pl}. The platform is loaded with the loading mass M_{pr}, which is damped from vibrations using the spring K_{pr}. F_g, force acting on the ground. The ground is represented by the adjoint mass M_{gr}, the spring by K_{gr}, and the damper by R_{gr}.

It follows that the accelerations are related by $-\ddot{U}_i/\ddot{U}_{pl} \approx M_{pl}/M_i$, meaning that the force acting on the ground is $F_{gr}(t) \approx 0$. In the interval $0 < t \leq t_1$, the spring K_{gr1} contracts fully, and the platform M_{pl} encounters the stiff spring K_{gr2}. The quantity $|\ddot{U}_{pl}|$ decreases (compared with the case of no contact with the ground), and we have a nonzero vertical force $F_{gr}(t) = M_i\ddot{U}_i + M_{pl}\ddot{U}_{pl}$. (In practice, for a good model of the ground, many springs are needed.) Knowing the force $F_{gr}(t)$ is important because, in a homogeneous half-space at depth z, the displacement of a longitudinal wave far from the source is given (see Chichinin [1984], p. 72) by $U_z^p = F_{gr}(f)/(2\pi\rho_g V_p^2 \cdot z)$, where ρ_g, V_p are the density of the medium and the velocity of the longitudinal wave, respectively, and $F_{gr}(f)$ is the amplitude of the force $F_{gr}(t)$ at a frequency f. This equation holds while $D \leq \lambda/4$, where D is the dimension of the source (its maximal length or width) and

$\lambda = V_p/f$ is the longitudinal wavelength. The formula is remarkable in that although $D \leq \lambda/4$ (and this often holds), the displacement U_z^p does not depend on the area or shape of the surface.

Electric Analog of the Mechanical Model

In studying the vibrational impact on a medium, equation (1) holds as well. It is enlightening to consider the well-known analogy between mechanical and electrical systems by applying Gamburtsev's method (Gamburtsev, 1959) (see Fig. 13b).

First, we consider the simplified case, in which the parameters of the mechanical structure (K_{gr}, R_{gr}, K_{pr}, etc.) are constant over time. In the electrical system, masses are replaced by inductances, the dampers by resistances, springs by capacitances, forces by voltages, and velocity by current. In this design, we may trace a circuit across the inductances M_i, M_{pr}, M_{pl} and through the complex impedance

$$Z_{gr} = j\omega M_{gr} + (1/(j\omega))K_{gr} + R_{gr}. \quad (A2)$$

The equation for voltage in this circuit is $F_i + F_{pr} + F_{pl} + F_{gr} = 0$. We may then write this equation in terms of impedances and currents. Voltage across the inductances M_i will be $F_i = j\omega M_i \cdot J_i = j\omega M_i \cdot \dot{U}_i = M_i \cdot \ddot{U}_i$, where $\dot{U}_i$ and $\ddot{U}_i$ denote the complex amplitudes of the velocity and acceleration of the inertial mass M_i, respectively, $\dot{U}_i \equiv J_i$. In this notation, $-j\omega M_i \cdot J_i + j\omega M_{pr} \cdot J_{pr} + j\omega M_{pl} \cdot J_{pl} + Z_g \cdot J_{pl} = 0 \rightarrow -M_i\ddot{U}_i + M_{pr}\ddot{U}_{pr} + M_{pl}\ddot{U}_{pl} - F_{gr} = 0$. This is precisely equation (1). The force F_{gr}, acting on the ground should have a negative sign, so that $F_{gr} = -Z_g \cdot J_{pl}$. The force of gravity can be accounted for in the model (see Fig. 13b) in the following manner (Chichinin, 1984): Sources of constant voltage $F_i^o = gM_i$, $F_{pr}^o = gM_{pr}$ and $F_{pl}^o = gM_{pl}$ are put in a series with inductances. The internal resistances of these sources are equal to zero, and their polarities are set in the direction of the current in the contour $Z_iZ_{pr}Z_{pl}$ on the circuit of Figure 13c. The constant force acting on the ground is

$$F_{gr}^o = F_i^o + F_{pr}^o + F_{pl}^o. \quad (A3)$$

The sources of constant voltage may be neglected when we work with alternating voltages and currents.

Principal Expressions

We need to determine the force F_{gr} acting on the ground in terms of the power-chamber force F_o and the various parameters of the source. For this purpose, we replace the loading system (see Fig. 13b) with a generalized impedance Z_{pr} (Fig. 13c), using the formula $\frac{1}{Z_{pr}} = \frac{1}{j\omega M_{pr}} + \frac{1}{K_{pr}/(j\omega) + R_{pr}}$.

It follows that

$$Z_{pr} = j\omega M_{pr} \cdot \frac{1 + j\omega R_{pr}K_{pr}}{1 - w^2M_{pr}/K_{pr} + j\omega R_{pr}/K_{pr}}, \quad (A4)$$

or

$$Z_{pr} = j\omega M_{pr} \cdot Z_{pr}^{oo}, \quad (A5)$$

$$Z_{pr}^{oo} = \frac{1 + ja_{pr}(f/f_{pr})}{1 - f^2/f_{pr}^2 + ja_{pr}(f/f_{pr})}, \quad (A6)$$

where

$$f_{pr} = (K_{pr}/M_{pr})^{1/2}/(2\pi), \quad (A7)$$

$$a_{pr} = 2\pi f_{pr} + \frac{R_{pr}}{K_{pr}} = \frac{R_{pr}}{2\pi f_{pr}M_{pr}}; \quad (A8)$$

where f_{pr} is resonant frequency and a_{pr} is the decay coefficient of the pressing system.

Using generalized impedances Z_{pr}, Z_{gr} (equations 5 and 2) and $Z_{pl} = j\omega M_{pl}$ simplifies the diagram in Figure 13b (see Fig. 13c). It can be seen, that the "current" J_{pl} and "voltage" F_{gr} according to Ohm's law are

$$J_{pl} = F_o/Z_s, \quad Z_s = Z_{pr} + Z_{pl} + Z_{gr},$$

$$F_{gr} = F_o \cdot Z_{gr}/Z_s. \quad (A9)$$

Now, we express the impedance Z_{gr} (see equation 2) as

$$Z_{gr} = K_{gr}/(j\omega) \cdot (-\omega^2M_{gr}/K_{gr} + 1 + j\omega R_{gr}/K_{gr})$$

through resonant frequency f_{oo} of the spring K_{gr}, with the mass M_{gr}, and through resonant frequency f_o of the spring K_{gr} with the mass $M_{gr} + M_{pl}$, decay coefficient a_{gr}:

$$Z_{gr} = K_{gr}/(j\omega) \cdot Z_o\mathrm{gr},$$

$$Z_{gr}^o = 1 - (f/f_{oo})^2 + ja_{gr}\, f/f_o, \quad (A10)$$

where

$$f_{oo} = (K_{gr}/M_{gr})^{1/2}/(2\pi), \quad (A11)$$

$$f_o = (K_{gr}/(M_{gr} + M_{pl}))^{1/2}/(2\pi), \quad a_{gr} = 2\pi f_o R_{gr}/K_{gr}.$$

Similarly, for

$$Z_{pl} + Z_{gr} = j\omega M_{pl} + j\omega M_{gr} + 1/(j\omega) \cdot K_{gr} + R_{gr}$$

we have

$$Z_{pl} + Z_g = K_{gr}/(j\omega) + (Z^o_{pl} + Z^o_{gr}),$$

$$Z^o_{pl} + Z^o_{gr} = 1 - (f/f_o)^2 + ja_{gr} \cdot f/f_o. \quad \text{(A12)}$$

The overall impedance $Z_s = Z_{pr} + Z_{pl} + Z_{gr}$ in the same form is

$$Z_s = K_{gr}/(j\omega) \cdot Z^o_s,$$

where $Z^o_s = Z^o_{pr} + Z^o_{pl} + Z^o_{gr}$.

The impedance $Z_{pr} = j\omega M_{pr} Z^{oo}_{pr}$ takes the form

$$Z_{pr} = K_{gr}/(j\omega) \cdot Z^o_{pr},$$

$$Z^o_{pr} = -\omega^2 M_{pr}/K_{gr} \cdot Z^{oo}_{pr}, \quad \text{(A13)}$$

where Z^{oo}_{pr} is given by equation (6). Substitution of equation (6) into expression (13) for Z^o_{pr} yields

$$Z^o_{pr} = -(f/f_{prg})^2 \cdot \frac{1 + ja_{pr}(f/f_{pr})}{1 - f^2/f^2_{pr} + ja_{pr}(f/f_{pr})}, \quad \text{(A14)}$$

where $f_{prg} = (K_{gr}/M_{pr})^{1/2}/(2\pi)$.

The force acting on the ground is expressed as

$$F_{gr} = F_o \cdot Z_{gr}/Z_s = F_o \cdot Z^o_{gr}/Z^o_s. \quad \text{(A15)}$$

The values of Z^o_{gr}, $Z^o_{gr} + Z^o_{pl}$, Z^o_{pr} are specified by the formulas (10), (12), and (14). As a result, the force $F_g r$ is expressed in terms of the resonant frequencies of the vibrator-ground system.

To find the resonant frequencies f_o, f_{oo}, f_{prg} of the spring K_{gr} with masses M_{gr}, $M_{pl} + M_{gr}$, M_{pr}, the value of K_{gr} must be estimated carefully. It is well known that the resonance frequency of a seismic-prospecting vibrator, standing on a compact ground road, is approximately equal to 30 Hz. This frequency (denote it f_1) is related to the spring K_{gr1} and masses M_{gr1}, M_{pl1} by the formula

$$\omega_1^2 = K_{gr1}/(M_{pl1} + M_{gr1}),$$

while

$$K_{gr1} = \omega_1^2 \cdot (M_{pl1} + M_{gr1}), \quad \text{(A16)}$$

where K_{gr1} is a ground stiffness for the seismic-prospecting vibrator, M_{pl1} is the platform mass, and M_{gr1} is the "associated mass" of the ground for this vibrator. (For more details on M_{gr1}, see Appendix B and therein equation 22.) It is obvious that f_1 will not be equal to 30 Hz on some other ground. This value quite easily and reliably can be found from the experiment.

The stiffness of the ground can be determined from the formula $K_{gr} = \Phi \cdot (S_{pl})^{1/2}$, where S_{pl} is the platform area, Φ is a certain quantity, independent of platform size. It can be determined from the data for a seismic-prospecting vibrator, that $\Phi = K_{g1}/(S_{pl1})^{1/2}$. Then,

$$K_{gr} = \Phi \cdot (S_{pl})^{1/2} = K_{gr1} \cdot S^{1/2}_{pl}/S^{1/2}_{pl1}$$

As a result of equations (16) and $(S_{pl}/S_{pl1})^{1/2} = r_o/r_{o1}$, where r_o, r_{o1} are equivalent radii of platforms,

$$K_{gr} = \omega_1^2 \cdot (M_{pl1} + M_{gr1}) \cdot r_o/r_{o1}. \quad \text{(A17)}$$

Substitution of equation (17) into equation (15) for the force F_{gr}, yields the following expression for the force acting on the ground:

$$F_{gr}(f) = F_o \frac{1 - (f/f_{oo})^2 + ja_{gr} f/f_o}{-(f/f_1)^2 \frac{M_{pr}}{M_{pl1} + M_{gr1}} Z^{oo}_{pr} + [1-(f/f_o)^2 + ja_{gr} f/f_o]}, \quad \text{(A18)}$$

where

$$f^2_{oo} = f_1^2 \frac{M_{pl1} + M_{gr1}}{M_{gr}} \cdot \frac{r_o}{r_{o1}},$$

$$f^2_o = f_1^2 \frac{M_{pl1} + M_{gr1}}{M_{pl} + M_{gr}} \cdot \frac{r_o}{r_{o1}},$$

$$a_{gr}/f_o = \frac{R_{gr}}{2\pi f_1^2 (M_{pl1} + M_{gr1})} \cdot \frac{r_{o1}}{r_o},$$

$$Z^{oo}_{pr} = \frac{1 + ja^{pr}(f/f_{pr})}{1 - f^2/f_{pr} + ja_{pr}(f/f_{pr})}.$$

The expression for Z^{oo}_{pr} is given in equation (6), where the resonant frequency f_{pr} and decay coefficient a_{pr} are shown to be related to parameters of the loading system M_{pr}, R_{pr}, K_{pr} (equations 4 and 5).

Thus, to calculate the force $F_{gr}(f)$ using equation (18), one needs to know the force F_o, the masses M_{gr}, M_{pr}, M_{pl} and the equivalent radius r_o of the platform; the parameters of the reference seismic-prospecting vibrator f_1, M_{pl1}, M_{gr1}, r_{o1}; the decay coefficients a_{gr}, a_{pr}; and the resonance frequency f_{pr}.

Appendix B
Vibrator-Ground System Characteristics

Power Chamber Force

Consider the problem of determining the force F_o, that is, an amplitude of the power chamber force.

In Figure 13, there is a damper R_o parallel to the power chamber. This is the internal resistance of the power chamber. If it did not exist, then as $M_i \to 0$, the acceleration $\ddot{U}_i(t)$ would grow without bound. Internal impedance is not necessarily real. The quantity $|Z_o|$ is small compared with the other resistances of the eccentric source. Hence, in our calculations we will take $Z_o = 0$.

Examining the diagrams in Figure 13b and c we clearly find that for the cases in which we can neglect the internal resistivity R_o of the force generator, the force F_o is equal to the force of the inertial mass M_i, that is, $F_o = F_i = j\omega M_i J_i = j\omega M_i \cdot j\omega U_i$, and

$$F_o = -\omega^2 U_i M_i. \tag{B1}$$

The maximum displacement amplitude $U_i^{(max)}$ of the inertial mass M_i is the most important parameter of any vibrator (hydraulic, eccentric, electrodynamic, etc.) that operates on the ground. When we say "the force amplitude of the power chamber or force generator is equal to the constant value F_o in the (f_{min}, f_{max}) frequency range," this means that for the frequency f_{min}, we have

$$|F_o| = \omega_{min}^2 U_i^{(max)} M_i. \tag{B2}$$

To provide F_o = constant for frequencies $\omega > \omega_{min}$, we must decrease the value of $U_i M_i$. This can be done in several ways. For example, in Vibrolocator, this decrease can be achieved by reducing the mass M_i. This mass is a fluid, which is capable of flowing through the special holes in the eccentric. In hydraulic vibrators, the value of U_i is reduced for this purpose.

Ground Parameters

In deriving equation (18), we use the parameters of the seismic-prospecting vibrator to determine the stiffness K_{gr} of the ground. To determine K_{gr} and other parameters of the impedance $Z_{gr} = j\omega M_{gr} + 1/j\omega \cdot K_{gr} + R_{gr}$ in a general case, we look to Chichinin (1984) and select the simplest case, namely the force uniformly distributed inside a circular area on the surface of a homogeneous half-space. The force F_{gr} is related to displacement U_{gr} of the ground ("immersion of the platform") by the formula $F_{gr}(t) = K_{gr}U_{gr}(t) + R_{gr}\dot{U}_{gr}(t) + M_{gr}\ddot{U}_{gr}(t)$. The term "immersion of the platform" means the displacement of the medium averaged over the surface of the circle area $S_{pl} = \pi r_o^2$ (r_o is the radius).

In spectral form, the equation for F_{gr} is

$$F_{gr}(\omega) = K_{gr}/(j\omega) \cdot I_{gr}(\omega) + R_{gr} \cdot I_{gr}(\omega) + j\omega M_{gr} \cdot I_{gr}(\omega), \tag{B3}$$

where $I_{gr}(\omega) \leftrightarrow \dot{U}_{gr}(t)$, and the ground parameters are

$$M_{gr} \approx (1 - \gamma^2)\rho r_o^3,\ K_{gr} \approx 6(1 - \gamma^2)\rho V_s^2 r_o, \tag{B4}$$

$$R_{gr} \approx 4(1 - \gamma^2)\rho V_s r_o^2; \tag{B5}$$

Here, V_p, V_s, ρ are the P and S velocities and the density of the elastic medium, $\gamma = V_s/V_p$ and r_o is the radius of the platform.

These equations are useful as approximate evaluations of impedances: the impedance of the associated mass M_{gr}, the stiffness impedance K_{gr} of the contact between platform and the ground, and the friction impedance R_{gr}. The energy $W = (1/2)\ R_{gr}|J_{gr}|^2$, which is released at R_{gr}, is the energy of generated seismic waves. For practical purposes, we also need to include the energy lost as heat. The value of stiffness K_{gr} is defined by properties of the ground at depths $z = 0 - r_o$. In particular, this value depends on V_s^2. But it is difficult to measure V_s at small distances ($z = 0 - r_o$), because the uppermost ground is very soft. Designers of building foundations find V_s by using immersion depth.

In Chichinin (1984) there are data taken from the handbooks of road builders that show that when the platform area is $S = 1 - 2\ m^2$, in typical compacted soils, the mass $M_{pl} = (1 - 2) \cdot 10^3$ kg has a resonance (with the spring K_g) at frequency $f_{pl} = (20 - 40)$ Hz.

Despite all these uncertainties, these formulas are very useful for understanding experimental results and predicting the dependence of source characteristics on medium parameters.

Platform Oscillations

In Figure 13b it is assumed that $J_{gr} = J_{pl}$ or $U_{gr} = U_{pl}$; in other words, the displacement of the ground under the platform coincides with the displacement of the platform. This is not entirely accurate. In practice, it is desirable that the static load force (the weight F_{pr}^o) be larger than the amplitude of F_o, the force generated by the power chamber, to maintain the contact between the platform and the ground. Despite this, the vibrations of the platform are not sinusoidal, because the ground should be modeled not as a single spring but as a chain of springs, as was done during the consideration of the impulse source.

During vibration, the discrepancy between U_{pl} and the sinusoid is easily measurable in an impulse seismogram constructed from seismic vibrations, with the main sweep-signal $b_1(t) = b_{10} \sin(\alpha t^2)$, and seismograms constructed from sweep-signals of the form $b_n(t) = b_{n0} \sin(n \cdot \alpha t^2)$. The amplitude of the second harmonic is only rarely larger than 1/10 of the amplitude of the principal mode; the amplitudes

of the third and other harmonics are usually even weaker. These weaker harmonics may be used in some studies that are outside of the scope of this article.

Another interesting effect arises when the seismogram is made with the aid of a sweep-signal of $n = 1/2$ or $n = 1/3$, which usually generates a low signal-to-noise ratio seismogram. Chichinin (1984) provides the following explanation. Suppose that the source is generating a signal of 10 Hz. If the quantity $F_o/F_{pr}^o \approx 3$ (where F_{pr}^o is the static load force that holds the platform to the ground and F_o is the amplitude of the force generated by the power chamber), the platform will jump up and down (striking the ground) with a frequency of 5 Hz. If on the other hand, $F_o/F_{pr}^o \approx 4 - 5$, the platform will strike the ground with a frequency of 10/3 Hz. If we further increase the ratio F_o/F_{pr}^o, then the frequency will decrease even more. In principle, this phenomenon may be exploited in constructing a low-frequency source, which would require a very strong power chamber.

To explain the experimental facts of seismogram generation after convolution with $n = 1/2$ or $n = 1/3$ when $F_o/F_{pr}^o \approx 1$, we should take into account that oscillations at 5, 10/3, . . . Hz may already be visible when $F_o/F_{pr}^o \approx 1$.

Below we neglect the previously mentioned weak effects and assume that $F_o/F_{pr}^o \leq 1$, that the soil can be described by a constant stiffness K_{gr}, and that the platform does not detach from the ground ($J_{gr} = J_{pl}$ or $U_{gr} = U_{pl}$).

In equation (18), the dimensionless parameter a_{gr}, is called the attenuation coefficient. Clues for finding this parameter are as follows. In seismic-prospecting vibrators, when $a_{gr} = 1/2$ in the vicinity of the resonance frequency ($f \approx f_1$), the theoretical value of the force is $F_{gr} \approx 2 \cdot F_o$. If the static force F_{gr}^o of the vibrator load to the ground is $F_{gr}^o \approx F_o$, then the platform detaches from the ground for a significant period. The corresponding nonlinearity effects can be easily removed from the data and therefore do not present a significant problem. However, some vibrators can be damaged by these detachments due to synchronism. Therefore, it is recommended to keep the condition $F_{gr}^o \approx 1.5 \cdot F_o$. Under this condition, the platform can also have slight insignificant detachments, which do not affect the vibrator itself. Based on this we can conclude that for typical soils $a_{gr} > 1/2$, since if we have $a_{gr} = 1/4$, then in the resonance regime ($f \approx f_1 = f_o$; see equation 18) the force is equal to $F_{gr} \approx 4 \cdot F_o$ and the recommendation $F_{gr}^o \approx 1.5 \cdot F_o$ does not help. (We are compelled to use such clues because it is practically impossible to accurately measure the force $F_{gr}(t)$ under the platform. To detect disconnection of the platform from the ground is also very difficult. The oscillograms of the experiment allow us to see deviations of the signal from a pure sinusoid, which are always present to some extent. Therefore, by saying that platform is detached or connected to the ground, we mean that for the ideal contact, the sinusoidal force $F_o(t)$ generates the sinusoidal displacement $U_{pl}(t)$. The expression "significant detachment" means that the main harmonic on the oscillogram $b_n(t) = b_{no} \sin(n\alpha t^2)$, $n = 1$, is barely seen in the background of $n > 1$ oscillations.)

Appendix C
Mobile Sources for Active Seismology

We consider a mobile 50-ton source, with a net weight of about 60 tons. The specifics of active seismology problems are such that the distance between sources may be on the order of hundreds of kilometers. To transport the source across such distances, over country roads and bridges of low weight tolerance, it is desirable that the weight of each separately transportable unit be no more than 15–20 tons. Hence, in its mobile state the discussed vibrator comprises a number of all-terrain vehicles carrying pieces of the source. The assembly of the source happens on location within 2–3 hr, with the aid of a specialized mobile crane. Keeping in mind that points of recording are located 200–300 km away, it is clear that the organization of field work is different from survey work, in which distances between source locations fall in the 50–100 m range.

Suppose a mobile vibrator is assembled on a location previously occupied by a seismic survey vibrator; it has the same platform area $S_{pl} = 2$ m^2, but the mass of the platform is $M_{pl} = 7 \cdot 10^3$ kg. The power chamber of this source generates the amplitude of 50 tons in a frequency range of 2 to 15 Hz. This means that for frequencies $f > 2$ Hz, the quantity $\omega^2 U_i M_i$ is maintained at 50 tons by decreasing the quantity $U_i M_i$. For frequencies $f < 2$ Hz, the quantity $U_i M_i = U_i^{(max)}$, $M_i =$ constant, and the force $F_o = \omega^2 U_i^{(max)} M_i$ decreases as $\sim f^2$.

The force acting on the ground can be estimated by using the formula in equation (18) derived in Appendix A. Calculations are carried out for three cases of vibrator functioning: V1, V2, and V3. Parameter variance is given in Table 2. The remainder of the parameters are the same in all cases: for force chamber $F_o = 50$ ton, $M_i = 5000$ kg, $U_i^{max} = 0.625$ m; for reference seismic-prospecting vibrator, $f_1 = 30$ Hz, $M_{pl1} = 2000$ kg, $S_{pl1} = 2$ m^2, $r_{o1} = 0.8$ m, $M_{gr1} = 500$ kg; for pressing and ground systems $f_{oo} = 67$ Hz, $a_{pr} = 1/20$, $M_{gr} = 500$ kg, $a_{gr} = 1$.

In cases V1 and V2, the pressing system carries a load of $M_{pr} = 5 \cdot 10^4$ kg. It is disjoined from the oscillations of the platform by a spring of stiffness K_{pr}. The resonance of load M_{pr} with the spring K_{pr} occurs at the frequency $f_{pr} = 1$ Hz in case V1 and at a frequency of about $f_{pr} = 2$ Hz in

Table 2
Parameters of Vibrator Functioning

Case	f_{pr} (Hz)	f_o (Hz)	M_{pr} (kg)	M_{pl} (kg)
V1	1	17	$50 \cdot 10^3$	$7 \cdot 10^3$
V2	2	17	$50 \cdot 10^3$	$7 \cdot 10^3$
V3	–	6.3	0	$57 \cdot 10^3$

case V2. In case V2, cheaper springs are installed in the load system.

The resonant frequency in cases V1 and V2 is equal to $f_o = f_1\,[(M_{plI} + M_{gr})/(M_{pl} + M_{gr})]^{1/2}) = 30 \cdot [(2000 + 500)/(7000 + 500)]^{1/2} \approx 17$ Hz. In case V3, where $M_{pl} = 57 \cdot 10^3$ kg, this frequency f_o will be equal to 6.3 Hz. Case V1 is designed to operate in a frequency range from 2 to 15 Hz, and case V2 is intended for operating at frequencies from 4 to 15 Hz. In case V3, the spring K_{pr} is blocked by a rigid rod, and the working range is planned to be from 2 to 5 Hz.

The graphs for cases V1, V2, V3 are plotted in Figure 14. For more details, Table 3 gives the values of the force F_{gr} at some chosen frequencies.

Judging from the spectra $F_{gr}(f)$ in Figure 14 and Table 3, one can see that in the full frequency range (1.5–15 Hz) the best fit is curve V1. Unfortunately, in case V1 the expensive springs must be used. Cheaper springs, which disjoin railway cars (of 50–70 tons) from vibration, are widely used in rail transport. The resonance frequency of such springs with masses of 50–70 ton is 2–3 Hz. Using these springs, we arrive at case V2, for which at frequencies $f \approx f_{pr}$ ($f_{pr} = 2$ Hz), the force F_{gr} is too small. (See Table 3, where it is shown that $F_{gr} = 23$ tons rather than the 49 tons of case V1.) The formulas (6) and (18) show that whereas $f/f_{pr} = 1$ we can even have $Z_{pr}^{oo} \to \infty$ and, therefore, $F_{gr} = 0$ if $a_{pr} \to 0$.

Consequently, to gain a sufficient force amplitude F_{gr} at low frequencies and within the whole working range (1.5–15 Hz), we can combine cases V2 and V3. Then we have the maximum amplitudes in the middle of the frequency interval and the sufficiently large amplitudes on both extremes.

Application of cases V2 and V3 requires that in every source location the vibrator must be operated twice. Afterward, during data processing, these two seismograms are sewn together. The resulting seismogram is the same as it would have been if the source operated over the full 1.5–15 Hz range without interruption.

The dependence of $F_{gr}(f)$ on different values of a_{pr}, that is, the attenuation coefficient of the pressing system, was also studied. This dependence is insignificant for a_{pr} in the (1/20, 1) range. For example, in case V1 at the frequency $f = 8$ Hz we have $F_{gr} = 58$ ton at $a_{pr} = 1/20$ and if $a_{pr} = 1$ we obtain $F_{gr} = 54$ tons. The static force (3) acting on the ground under the platform is $F_{gr}^{o} = 62$ tons. At those fre-

Table 3

Force F_{gr} versus Frequency for Variants V1, V2, V3

Case	Frequency (Hz)	1	1.5	2	4	8	16	20
V1	Force F_{gr} (ton)	11	27	49	51	58	68	59
V2		12.7	31	23	46	54	66	59
V3		12.7	29	55	69	53	21	16

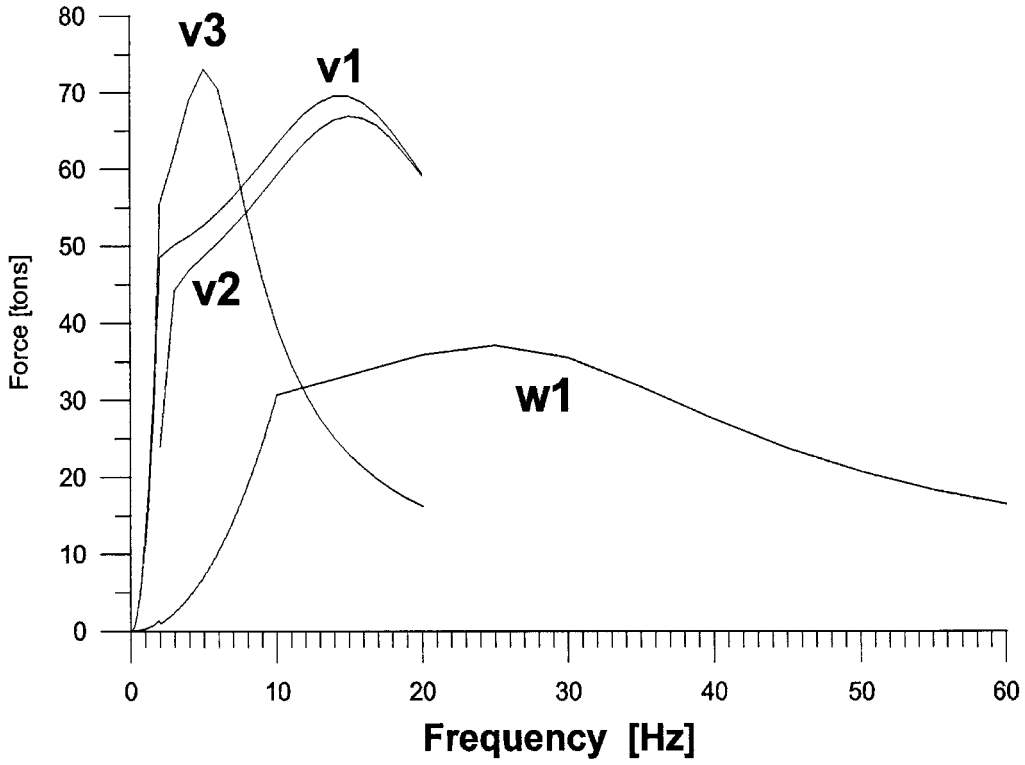

Figure 14. Theoretical force amplitude generated by the low-frequency transportable LEV for cases V1, V2, and V3, and by the hydraulic seismic prospecting vibrator (W1).

quencies when $F_{gr} > F^{o}_{gr}$, a small space should appear between the platform and the ground. For the LEV this is not a major problem.

Sometimes the question arises, can one use the seismic survey vibrator in active seismology? To answer this question, it is instructive to explore the radiation of the previously discussed seismic survey vibrator in the range of frequencies below 10 Hz, though this source is not intended for frequencies of this range. For this vibrator, the force amplitude of the power chamber is equal to $F_{o1} = 30$ tons in the range of frequencies from $f_{min} = 10$ to $f = 210$ Hz, $M_i = 2000$ kg. This means, by formulas (19), (20) that $U_i^{(max)} = F_{o1}\omega_{min}^2 M_i^{-1} = 3.77$ cm. For frequencies up to 10 Hz, the force of the generator will be described by the equation $F_o = \omega^2 U_i^{(max)} M_i$. We substitute this into equation (18) to determine the force acting on the ground F_{gr}, for frequencies up to 10 Hz. The other parameters are: $f_o = 30$ Hz, $a_{gr} = 1$, $S_{pl} = 2$ m^2, $M_{pr} = 30 \cdot 10^3$ kg, $f_{pr} = 2$ Hz, $a_{pr} = 0.1$. Then, the graph for the previously, discussed seismic-prospecting vibrator appears as curve W1 in Figure 14.

Calculation gives the following result: When the frequency f grows to 9 Hz, the force F_{gr} grows as $\sim 0.3f^2$ until 25 tons at $f = 9$ Hz; then the force $F_{gr}(f)$ grows slowly until reaching its maximum at $f \approx 25$ Hz, after which it decreases taking the values 16 tons at $f = 60$ Hz, 10 tons at $f = 100$ Hz, and 7 tons at $f = 210$ Hz.

In this example, the static force on the ground is $F^{o}_{gr} = 34$ tons. Hence, for frequencies where $F_{gr} > F^{o}_{gr}$, the form of the displacement of the ground under the vibrator will differ slightly from a sinusoid. Resulting harmonics can be easily extracted through subsequent convolution. The increased force F_{gr} at resonance leads to decreased force at high frequencies. To avoid this, the force F_o should be increased at higher frequencies.

In summary, for frequencies below 10 Hz, the vibrator still operates, but the force acting on the ground is fairly small.

Institute of Computational Mathematics and Mathematical Geophysics
Siberian Branch of Russian Academy of Sciences
Lavrentieva pr., 6
630090, Novosibirsk, Russia
alekseev@sscc.ru
(A.S.A.)

Institute of Geophysics
Siberian Branch of Russian Academy of Sciences
Koptuga pr., 3
630090, Novosibirsk, Russia
iro@online.sinor.ru
(I.S.C.)

Lawrence Berkeley National Laboratory
1 Cyclotron Road
Berkeley, California 94720
VAKorneev@lbl.gov
(V.A.K.)

Manuscript received 22 December 2003.